Monitoring of silicone adhesive in space solar cells with an embedded multi-parameter TFBG sensor in a simulated space environment

OPEN ACCESS
IOP Publishing
Measurement Science and Technology
Meas. Sci. Technol. **33** (2022) 085108 (9pp)
https://doi.org/10.1088/1361-6501/ac6d45

Monitoring of silicone adhesive in space solar cells with an embedded multi-parameter TFBG sensor in a simulated space environment

Luigi Fazzi[1,2,*], Nuno Dias[2], Malgorzata Holynska[2], Adrian Tighe[2], Riccardo Rampini[2] and Roger M Groves[1]

[1] Structural Integrity and Composites Group, Faculty of Aerospace Engineering, Delft University of Technology, Delft 2629 HS, The Netherlands
[2] ESA-ESTEC, TEC-QEE, Keplerlaan 1, 2200 AZ Noordwijk, The Netherlands

E-mail: l.fazzi@tudelft.nl and luigi.fazzi@esa.int

Received 7 December 2021, revised 28 February 2022
Accepted for publication 5 May 2022
Published 13 May 2022

Abstract

In this research the ageing of a silicone adhesive in a simulated space environment is monitored through an embedded three parameter tilted fibre Bragg grating (TFBG) sensor. Here, the silicone is used as an adhesive between two thin cover glasses, and the space environmental ageing is simulated by thermal cycles in high vacuum conditions (better than 10^{-5} mbar). These operational conditions can induce variations in the silicone adhesive with respect to its original properties such as dimensional stability, chemical composition, generated contaminants, discoloration and, mechanical or optical degradation. Therefore, surrounded by the adhesive, in the centre of the cover glass sandwich, a weakly tilted FBG sensor was placed to obtain information from its spectra on the state of the polymer during the test. Specifically, the temperature, strain and refractive index (RI) of the silicone can be, simultaneously and separately, measured from the spectrum of a single TFBG from selected resonance peaks. These parameters can be used to evaluate the 'health' state of the silicone during the vacuum thermal cycles. The simultaneous TFBG thermomechanical measurements gave a solution to the non-localized measuring issues when using classical fibre optic or electrical strain-gauges and a thermocouple to compensate the temperature and to better understand the material behaviour. The trends of the measured parameters are reported during the entire testing time, and at the end of the test, the optical fibre sensor measured a negative strain of ∼100 με and a positive RI variation of ∼0.002.

Keywords: TFBG, silicone, degradation, thermal cycles, space environment

(Some figures may appear in colour only in the online journal)

* Author to whom any correspondence should be addressed.

1. Introduction

The space environment may expose satellite components, structures or systems to severe operational conditions such as high vacuum, ultra-violet (UV) and ionizing radiations, thermal cycles, micro-gravity, atomic oxygen (ATOX), high accelerations, vibrations and space debris. Due to each harsh perturbation or a combination of these, the original state and properties of the used materials can be influenced and modified [1].

Silicone materials are organic polymers widely used in spacecraft and satellites as adhesives, sealants, release coatings, lubricants and encapsulants for several applications, like in solar cells or as potting compounds [2]. Indeed, they offer attractive and versatile properties for space technologies, such as low glass transition temperature, low outgassing, good thermal stability and excellent elastomeric properties in combination with optical transparency [3].

However, high vacuum induces polymer outgassing of additives and low-molecular weight residues, affecting the original dimensional stability and composition of the material as well as depositing contaminants on nearby cold surfaces. In addition, the interaction of the contaminant layers, with UV or ionizing radiation, thermal cycles and ATOX can cause their fixation causing severe issues [4].

Many space missions also include rapid thermal excursions and cycles, for example in the case of Earth orbital missions, spacecraft and satellites pass from sunlight to shadow cycling based on their orbit. Typical temperature fluctuations are between −100 °C to over 300 °C [2], which can strongly influence the polymers' mechanical performance during the mission lifetime. Another issue concerning this large temperature excursion regards the use of the silicone as an adhesive to bond elements of different nature, in case the coefficients of thermal expansion (CTEs) between the elements do not match each other, cracking is induced which weakens the bond strength. From the chemical point of view, high temperatures or severe thermal variations can induce new chemical reactions in organic molecules involving undesirable post-curing or ageing, rupture of bonds and discolouration of the material [5]. As a consequence, the silicone adhesive can lose its optical properties which originally made it extremely useful in space solar cells or other applications. These introduced effects can be caused only by high-vacuum and thermal cycles, however, in combination with other space environment factors makes the operational working conditions more severe.

For all these reasons, space materials are required to undergo strict testing campaigns to determine their suitability for space applications and to evaluate their behaviour and the consequences of space environment exposure [6]. In this way, premature failures and efficiency degradation can be minimised.

In this work, a multi-parameter embedded optical fibre (OF) sensor, based on a weakly tilted fibre Bragg grating (TFBG), is proposed to detect and monitor simultaneously the thermomechanical and chemical state of a silicone adhesive between two cover glasses, in a space environment simulated high vacuum thermal cycling test. The TFBG sensor satisfies the embedding requirements of low intrusiveness (Ø125 μm) and mass (∼65 g km^{-1}). Further, by performing some preliminary tests in our thermal and outgassing labs, the OF has been proven to be compatible with the simulated space environment. Each single TFBG sensor has been theoretically demonstrated to be able to measure simultaneously and separately strain, temperature and refractive index (RI) of the surrounding material [7]. While, in a real application, it was proven that this single sensor may be used to determine the thermomechanical state of a glass-fibre/epoxy composite when embedded inside [8].

In the present work, strain-temperature measurements with the OF sensor were used to monitor the change in the thermomechanical state of the silicone material induced by the thermal cycles. This data was also used to correct and compare with the deformation trend obtained by using the thermocouple (TC) temperature compensation of the TFBG spectrum, which is the classical strain-gauge approach. At the same time, silicone RI variations were observed, which enabled us to understand the possible changes of the original refractometric properties of the silicone material. In particular, the RI variations occurring in a polymeric material can be caused by post-curing [9, 10], ageing and degradation [11, 12] with the temperature variation. Hence, the silicone RI variation might indicate an evolution of the material, during the thermal cycles. To investigate further, differential scanning calorimetry (DSC) measurements were also performed.

2. TFBG sensing theory

TFBGs are tilted short period gratings manufactured with an inclination of the Bragg grating with respect with the optical axis of the OF. The most used manufacturing process to impose this special permanent modulation in the RI core of the OF, consists of using UV laser light passing through a phase-mask rotated with respect to the OF, one which can be also rotated with respect to the phase-mask [13]. The imposed inclination is called tilt angle (θ). Figure 1 shows a schematic of the internal structure of the TFBG sensor, where the grating period Λ_G along the OF axis and the nominal grating period $\Lambda = \Lambda_G \cos\theta$ are defined.

As easily noticeable from the previous picture, the tilt angle allows an enhancement of the cladding mode-coupling with the forward-propagating core mode. This results, in the sensor's transmission spectrum, of the generation of many close resonance peaks placed at lower wavelengths than the fundamental Bragg peak (which is usually the only resonance in the fibre Bragg grating (FBG) spectrum). In particular, in the case of weakly TFBG ($\theta \leqslant 15°$), which has been used in this work, three different kinds of peaks can be distinguished in the spectrum: the Bragg, the Ghost and the cladding peaks [14]. These appear in the transmission spectrum as figure 2 shows, and their sensing properties can be exploited to perform three parameter measurements with a single TFBG sensor. In fact, although the Bragg and Ghost peaks are susceptible to thermomechanical perturbations, they are immune to changes of the surrounding RI [15]. At the same time, the

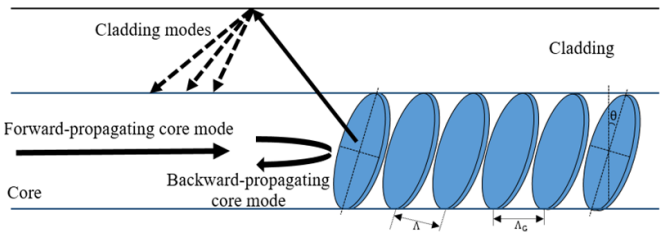

Figure 1. Schematic of a weakly TFBG internal structure.

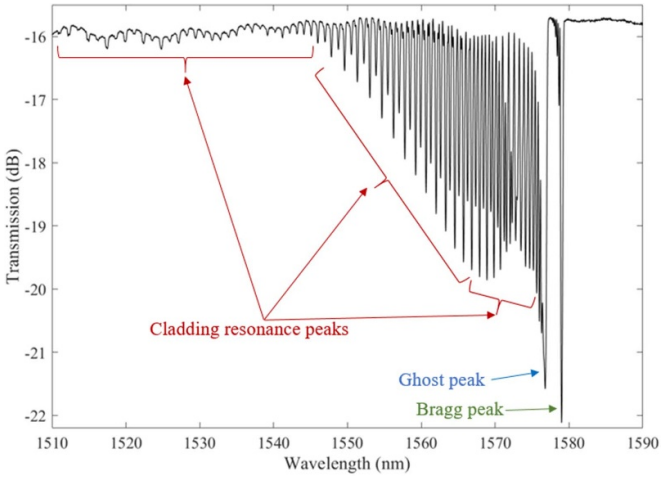

Figure 2. Typical weakly ($\theta = 3°$) TFBG transmission spectrum.

cladding resonances undergo a wavelength shift and amplitude change when the external RI is varying. Hence, by performing a preliminary calibration, both the Bragg and the Ghost peaks can be used to measure simultaneously and separately the temperature and the strain variation of the material where the sensor is embedded [8]. At the same time, the envelope area of the upper and lower cladding resonance peaks can be used to detect independently the RI variation of the medium surrounding the TFBG sensor [7, 14–16].

2.1. Strain-temperature and surrounding RI measurement techniques from TFBG spectrum

The measurement techniques of the three parameters require the thermomechanical and refractometric calibration of the sensor (section 3.1). Once this is completed, the following demodulation techniques can be applied to obtain the parameters' value from the TFBG spectrum.

The strain-temperature variations can be obtained from the spectrum by considering the wavelength shifting of any two selected resonance peaks. However, since the wavelength of the cladding modes is affected by the external RI, the Bragg and Ghost peaks are considered for such scope. As equation (1) [8] shows, the variation of the strain and temperature ($\Delta\varepsilon$,ΔT) can be found by calculating the matrix product of the inverse of the sensitivity matrix **K** and the Bragg and Ghost wavelength shifts ($\Delta\lambda_{\text{Bragg}}$,$\Delta\lambda_{\text{Ghost}}$) with respect to the starting condition

$$\begin{pmatrix} \Delta\lambda_{\text{Bragg}} \\ \Delta\lambda_{\text{Ghost}} \end{pmatrix} = \begin{pmatrix} K_{\varepsilon,\text{Bragg}} & K_{T,\text{Bragg}} \\ K_{\varepsilon,\text{Ghost}} & K_{T,\text{Ghost}} \end{pmatrix} \begin{pmatrix} \Delta\varepsilon \\ \Delta T \end{pmatrix} = \mathbf{K} \begin{pmatrix} \Delta\varepsilon \\ \Delta T \end{pmatrix} => \begin{pmatrix} \Delta\varepsilon \\ \Delta T \end{pmatrix} = \mathbf{K}^{-1} \begin{pmatrix} \Delta\lambda_{\text{Bragg}} \\ \Delta\lambda_{\text{Ghost}} \end{pmatrix}. \quad (1)$$

The sensitivity coefficients (K_ε,K_T) of the Bragg and Ghost peaks are obtained from the thermomechanical calibration of the TFBG. Since this technique is based on the wavelength variation of the selected peaks and the sensitivity coefficients that are used in combination in **K**, the proper calculation of variables depends on the thermal resolution (TR) of the TFBG. This is calculated through the ratio between the scanning wavelength resolution (swR) of the interrogator system used to acquire the TFBG spectra and $|K_{T,\text{Bragg}} - K_{T,\text{Ghost}}|$:

$$\text{TR} = \frac{\text{swR}}{|K_{T,\text{Bragg}} - K_{T,\text{Ghost}}|}. \quad (2)$$

The omission of the calculation which is respecting this constraint implies incorrect $\Delta\varepsilon$ and ΔT values. The strain resolution can be simply calculated by multiplying swR by K_ε. When equation (1) is used, the TFBG is also called a temperature self-compensated TFBG. While if the TC acquisitions are used to compensate the wavelength shift of a selected peak to obtain the strain level, then in this case the TFBG is used as a standard strain-gauge FBG sensor.

The demodulation of the TFBG spectrum to obtain the surrounding RI concerns the use of the Delaunay triangulation technique [15] to extract the envelope area of the upper and lower cladding resonance peaks. Once the envelope area value is obtained, it is normalised with respect with a reference area and inserted in a fitting correlation function which returns the surrounding RI. The fitting correlation function is determined during the refractometric calibration of the TFBG and it links the normalised envelope area values of the cladding peaks with the external RIs. More details are reported in the TFBG calibration section.

3. Methodology

The TFBG sensor and its interrogator system used in this work are described in section 3.1, while its thermomechanical and refractometric calibration are treated in sections 3.2 and 3.3. Section 3.4 is dedicated to the cover glass sandwich sample and testing facility description, specifically the materials, the dimensions and the components are described. The final section 3.5 details the parameters used to perform the thermal cycles under high vacuum environmental conditions.

3.1. Specifications of the embedded TFBG in simulated cover glass sandwich

The TFBG sensor embedded in the silicone adhesive was manufactured by FORC-Photonics in not-recoated (∼20 mm across the TFBG length) Fibercore PS1250/1500 OF using the rotated phase-mask technique. The sensor has a 3° tilt

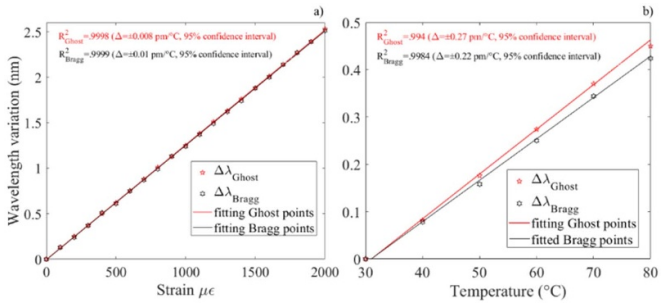

Figure 3. Trends of the wavelength variation for Bragg and Ghost peaks during (a) strain calibration and (b) thermal calibration of the TFBG.

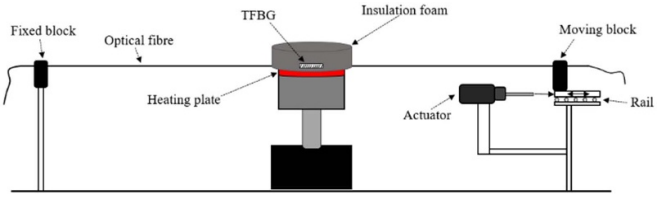

Figure 4. Schematic of the setup for thermomechanical calibration of the OF sensor.

angle and is 4 mm long. The coating comprises a layer of UV-cured acrylate. The TFBG was certified by the manufacturer to operate in a temperature range between −40 °C and 85 °C without degradation of the spectrum or the coating layer for long exposure time. During the entire calibration and testing stage, the TFBG spectra were always acquired using the NI PXI-4844 interrogator (swR = 4 pm, scanning accuracy ±1 pm and minimum power detection 6.103×10^{-4} dBm).

3.2. Thermomechanical calibration of the TFBG sensor

The sensitivity coefficients K_ε and K_T of the selected peaks (in this case, the Bragg and Ghost peaks) are necessarily determined by performing a thermomechanical calibration of the TFBG. For this purpose, a dedicated translation stage equipped with a Zaber NA34C60-T4 linear actuator (absolute accuracy 36 μm, relative accuracy ±2 μm) was used to increasingly apply an axial strain to a 1 m long OF. The sensor's spectra were recorded for each applied strain value. As shown in figure 3(a), the wavelength variation is linear with the increase of the deformation (which is also valid for the temperature in figure 3(b)). The calculated coefficients from the slopes of the linear fitting are $K_{\varepsilon,\mathrm{Bragg}} = 1.255 \pm 0.008$ pm $\mu\varepsilon^{-1}$ and $K_{\varepsilon,\mathrm{Ghost}} = 1.255 \pm 0.01$ pm $\mu\varepsilon^{-1}$. The accuracy of the coefficients takes into account also the repeatability of the measurements, specifically each deformation level was repeated 5 times.

The thermal calibration was also performed using the same translation stage, with a hot plate placed just below the TFBG sensor (see figure 4). A K-type TC sensor, with accuracy ±1 °C, was placed as close as possible to the sensor on the hotplate,, to measure the temperature. The entire apparatus was isolated from the surrounding environment with a foam insulation cover. The sensor was calibrated from 30 °C until 80 °C. From the slope of the linear fitting (figure 3(b)), the extracted sensitivity coefficients are $K_{T,\mathrm{Bragg}} = 8.96 \pm 0.22$ pm °C^{-1} and $K_{T,\mathrm{Ghost}} = 9.53 \pm 0.27$ pm °C^{-1}. Therefore, the TR of the TFBG sensor is ∼7 °C.

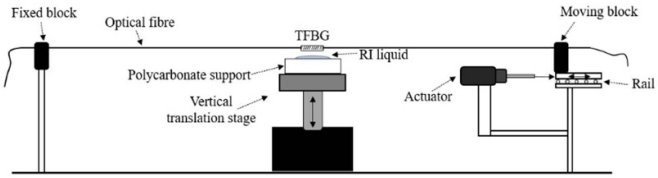

Figure 5. Schematic of the setup for RI calibration of the OF sensor.

3.3. RI calibration of the TFBG sensor

The refractometric calibration was performed using the setup shown in figure 5. Specifically, a set of Cargille RI oils (range: 1.3–1.7 ± 0.0002 between 18 °C and 30 °C) was used on top of a polycarbonate flat surface to immerse the sensor. The TFBG was held in a linear position by the translation stage and positioned just above the RI liquid. The full immersion of the TFBG inside the oils was induced by the vertical translation stage on which the polycarbonate surface was placed. Furthermore, a K-TC measured the temperature variations as close as possible to the TFBG, the temperature was kept at 20 ± 1.5 °C.

Once the TFBG spectra acquisition was completed, the spectra were demodulated using the D-T technique [15]. The envelope areas were then normalised with respect to the one obtained by immersing the TFBG at 1.32 RI, in this way the correlation points are found along the RI range as shown in figure 6. At this point, several fitting functions can be taken into account based on the correlation points trend by considering different degree of polynomial regression. For the silicone adhesive used in this study, the RI is around 1.43 [17], and considering the temperature range and the duration of the test, the minimum and maximum expected variations are within the 1.4–1.45 RI range. Hence, to optimise the RI measurement performance of the TFBG, the fitting correlation function was obtained inside this RI range. A study on the RI measurement performance was made as in [14]. Indeed, as a strain variation induces a shifting of the cladding peaks wavelength, it can comprise the accuracy of the measured RI by influencing the value of the envelope area. Therefore, the analysis was performed to calculate a standard deviation that considers also this kind of error. The R^2-error of the fitting is 0.9999 using a 4th degree polynomial function, with a maximum normalised area standard deviation of 0.0016 and a mean RI resolution of 2×10^{-7}.

The thermomechanical and refractometric calibration of the TFBG was performed at the non-destructive testing laboratory of the Aerospace Structures and Materials Department at TU Delft.

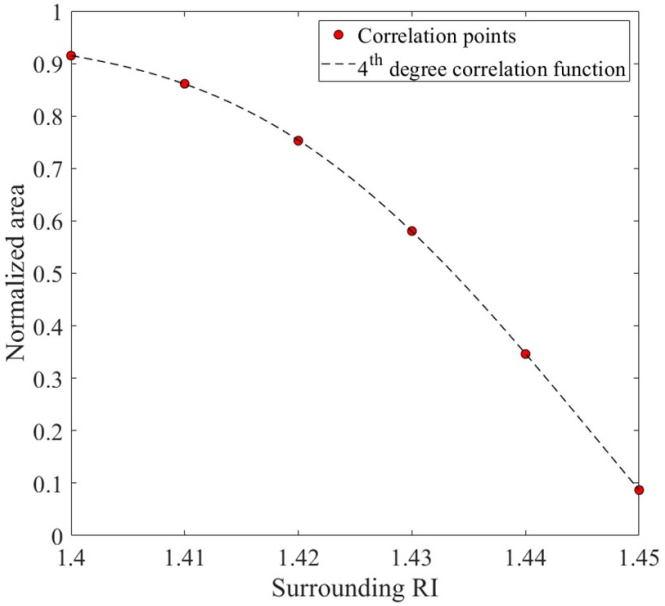

Figure 6. RI calibration points and fitting function in the RI range 1.4–1.45.

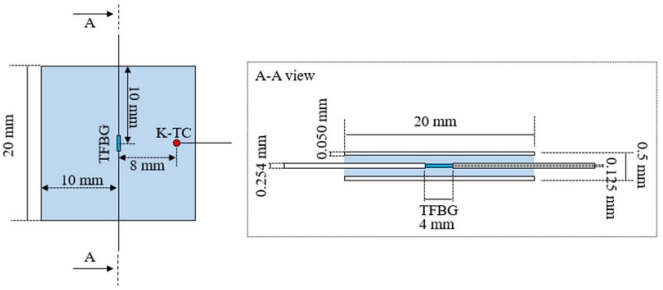

Figure 7. Schematic of TFBG sensorised cover glass sandwich sample design.

3.4. Sensorised cover glass sandwich sample and high vacuum thermal testing setup

The cover glass sandwich sample comprised Nusil^{TM} CV16-2500, a transparent optical adhesive, to bond together two layers of cerium doped microsheets cover glass (20 × 20 × 0.05 mm). These materials are typically used for space solar arrays to protect the solar cells from the space environment (for solar arrays, a single sheet of cover glass is bonded onto the cell surface). The TFBG sensor was embedded inside the adhesive during the manufacturing of the sample. The sensor is placed in the centre of the sandwich so that the OF is parallel to two sides and perpendicular to the other two (figure 7). A K-TC (Ø ≈ 100 µm) sensor was also embedded in the silicone adhesive to monitor the temperature trend during the test and to compare it with that measured by the TFBG sensor. Once the TFBG and the TC sensors were embedded and the silicone adhesive cured, the final thickness of the sample was about 0.5 mm.

The high vacuum thermal cycles were performed at the European Space Research and Technology Centre (ESTEC) with the MCross facility. This is a high vacuum testing

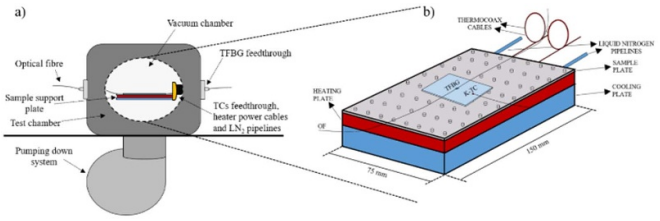

Figure 8. Schematic of the MCross facility: (a) the sample holder, (b) the heating and cooling plates.

chamber used to simulate the space environment, such as UV/VUV radiation, thermal cycling (fatigue) and long-term temperature ageing exposure of materials. For the scope of this work, the facility comprises a test chamber connected with a Pfeiffer Turbo Molecular pump and a membrane pump to create high vacuum down to 10^{-6} mbar. A metallic sample plate is placed on top of a resistance heating plate (thermocoax), which is mounted on a liquid nitrogen coolable plate (figures 8(a) and (b)). The chamber is also equipped with Kapton-coated K-type TCs, which can be attached to the sample or the plate for temperature monitoring. Furthermore, to acquire the spectra of the OF sensors, the facility was also upgraded with two hermetic polarization-maintaining fibre optic feedthroughs manufactured by SQS, each of which has two input/output FC/APC connectors, externally connected with two optical circulators, and hence, to the interrogator system.

The recommended temperature curing profile of the silicone adhesive comprises 4 h at 65 °C [17]. Curing was performed in an oven once the cover glass sandwich was assembled with the embedded sensors.

The DSC test was performed using a TA Instruments DSC 2500 machine at the thermal lab at ESTEC. The temperature range used for the DSC test was between −150 °C and 250 °C with a heating-up/cooling down ramp of 10 °C min^{-1} in nitrogen atmosphere.

3.5. High vacuum thermal cycling test parameters

The sample was clamped on the support plate using a few layers of Kapton® Polyimide tape to ensure good thermal contact between the elements. Indeed, since the test is performed in a vacuum environment, the contact quality is important to control the heat transfer between the heating/cooling plate and the sample. Once the cover glass sandwich was mounted on top of the sample support plate (figure 8(b)), the vacuum was achieved inside the chamber through the pumping down system. The data acquisition system of the TFBG sensor and the mounted TCs recorded the spectra and the temperature values during the entire exposure time. When the pressure inside the chamber reached ∼2 × 10^{-6} mbar, the heating plate was switched-on so that the thermal cycling started. At a certain time, after the stabilisation of the temperature, the heater was switched off and the cooler was activated to cool-down the sample. Through this cyclic temperature inversion, the sample

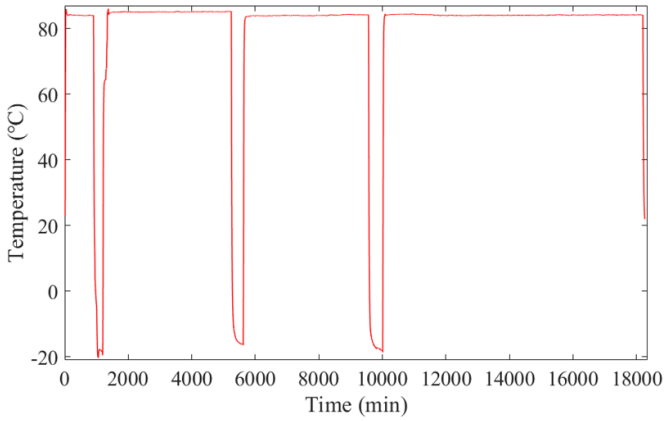

Figure 9. Temperature profile measured by the embedded TC during the test.

was exposed to thermal ageing cycles between ∼−20 °C and ∼85 °C, as shown in figure 9.

4. Results

In this section the strain-temperature and the RI measurements detected from the TFBG sensor in the silicone adhesive during the thermal cycle test are presented and commented.

An interesting aspect is the comparison between the strain values measured with the single self-temperature-compensated TFBG and those obtained using a classical approach by compensating the temperature effects on the TFBG spectrum using the TC measurements. Indeed, one of the most used previous techniques to compensate the cross-temperature sensitivity on the standard FBG sensors comprises the removal from the total Bragg wavelength shift of the part due to the temperature variation recorded with TC measurements [8]. While the TFBG measurements of the silicone RI highlighted a variation compared to the initial condition, which may be due to a physical properties evolution of the adhesive.

4.1. Classical approach: TC compensation measurements

As demonstrated in figure 10, the recorded Bragg peak wavelength variation and the TC temperature profile have some delays at different times. Hence, the compensation of the TFBG cross-temperature sensitivity using the TC measurements, specifically in a vacuum environment, suffers from non-localized measurements. This is due to the different location of the two sensors and an extremely non-homogeneous distribution of the temperature in vacuum. This implies that conduction can be considered as the only heat transfer mode, and this consequently, results in a delay in the sensitivity of sensors placed in different points. The delay can increase with the distance between the two sensors.

As a consequence, since the Bragg wavelength shift is not properly compensated in same range, the measured deformation curve has unexpected trends or inaccurate values as observed in figure 11. Moreover, since the test is performed

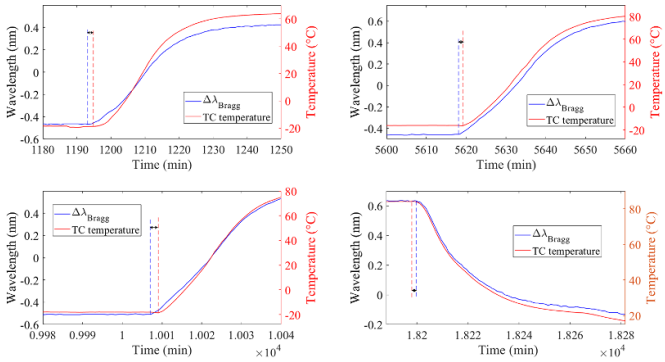

Figure 10. Comparion between the trends of the Bragg wavelength variation and temperature measured by TC during the experiment.

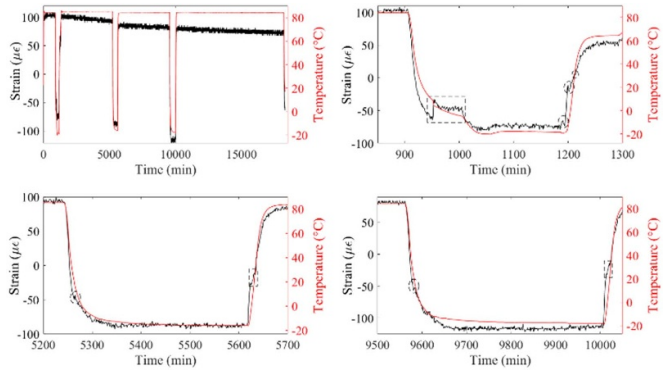

Figure 11. Strain values measured by compensation of the TFBG through TC temperature measurement.

in vacuum, the two different locations can experience different temperatures which means a possible wrong evaluation of the strain.

These issues can be overcome by using the TFBG as a dual parameter single sensor because, being self-compensated, the measurement is point-localized removing the delay between two different devices. The next section reports the results of the simultaneous strain-temperature measurements of the TFBG, showing that this sensor is promising for space environmental measurements under vacuum.

4.2. TFBG simultaneous strain-temperature measurements

Using the demodulation technique represented by equation (1) on the TFBG spectra, the strain-temperature variations can be calculated starting from a reference condition, which is considered as the switching-on moment of the heating plate. In figure 12, the strain and temperature trends measured with the single TFBG are reported, in blue and red, respectively, and compared with the curves obtained from the compensation of the Bragg wavelength shift with the TC measurements.

From figure 13, the silicone strain trend, measured with the self-compensated TFBG, does not show the unexpected spike or behavior which was seen using only the TC compensation (figure 11). Although the strain trends of the two different techniques are similar, the measured TFBG strains have a smoother and continuous trend, underlining the effectiveness

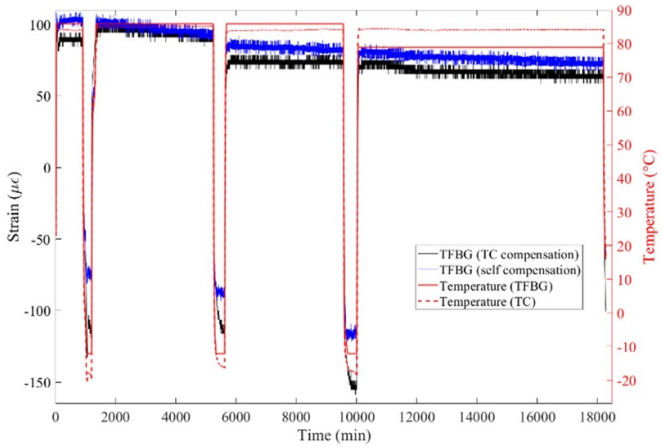

Figure 12. Strain values measured by self-compensated TFBG and comparison with the strain curve from figure 11.

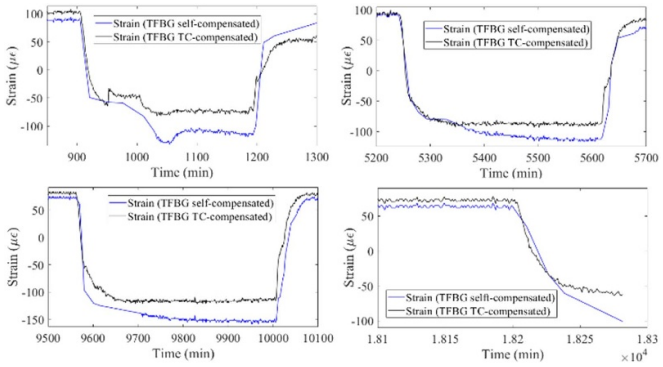

Figure 13. Strain curves during heating-up, cooling-down and final phases of figure 12.

of the self-compensated TFBG. The difference in strain and temperatures, even after the transient of thermal excursion, is due to the TR of the TFBG and the different embedding position of the two sensors. In fact, as introduced in section 2.1, the measurements of the strain are performed in accordance with the sensor's TR, this causes a strain accuracy of ± 12.8 με.

Regarding the thermomechanical state of the silicone adhesive during its ageing, the TFBG measurements suggest a permanent shrinkage of the material following the thermal cycles. Using both techniques, there is a consistent negative deformation state of 60.8 με at the same initial temperature (22.8 °C). This means that the silicone adhesive has undergone a change of its mechanical state, this could be by a combination of factors such as the variation of its physical state (due to post-curing, ageing) and (2) the different CTEs of the several materials that compose the sample.

4.3. Silicone adhesive RI variations detected by the TFBG

Simultaneously to strain and temperature, from the envelope area of the upper and lower cladding peaks in the TFBG spectrum, the silicone RI can be determined by applying the demodulation technique described in section 2.1. However, the same envelope area can give an indication of the surrounding

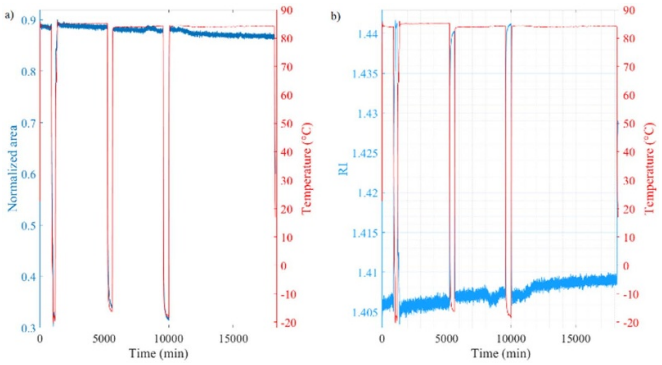

Figure 14. (a) Cladding resonance peaks envelope area trend and (b) silicone adhesive RI trend.

RI as it is dependent from this last one. The measured trends of the envelope area and RI of the silicone adhesive are reported in figures 14(a) and (b) during the entire testing time. It is evident from the calibration curve in figure 6, that the envelope area increases with increasing temperature, while it decreases during the cooling-down phase (figure 14(a)). The RI range given from the envelope area excursion is between 1.4 and 1.45, as expected (section 3.3). The evolution of the silicone RI shows expected behaviour with changing temperature. The initial silicone RI measured by the TFBG sensor was 1.42648 at 22.6 °C, which is close to the value declared by [17]. From this value, the RI changes according to the thermal and physical properties of the material where the TFBG is embedded [18]. At the end of the test, the envelope area and the RI were different with respect to their initial value at the same temperature. In particular, the envelope area reached a final variation of -2.1%, which in terms of RI means a value of 1.42744 at the same initial temperature. Now, considering the level of strain of the tested silicone at the same time, the error induced on the RI measurement is in the order of 10^{-5} [14], while that linked to the temperature is negligible. This implies that the silicone RI variation is fully induced by some physical or chemical processes generated in the material during the high vacuum thermal cycles.

For more accurate investigation, a DSC test was also performed on a sample of pure cured silicone material to detect eventual absorption or release of heat due to chemical reactions or physical processes (such as phase transitions) induced by temperature variations. The heat flow as a function of temperature variation during the DSC test is shown in figure 15.

The heat flow trend detected during the DSC test indicates exothermic (positive y-axis) and endothermic (negative y-axis) processes with the temperature evolution, suggesting that the thermal characteristics of the silicone may change due to temperature excursions. Furthermore, although the trend is reversible, some little spikes and bumps are present at several temperatures. These may suggest the generation of volatiles which release or absorb heat during the test due to different thermal conditions. The effect of volatiles evolution is expected to be even stronger in simulated space environments due to Le Chatelier's principle [19]. However, another aspect to consider regards the emission of volatile acetic acid from the

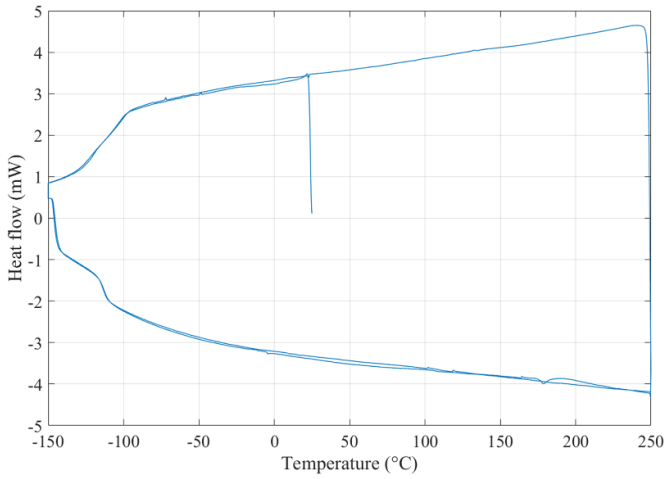

Figure 15. Heat flow and temperature measured during the DSC test on the silicone sample before thermal cycling test.

silicone adhesive during the (post-) curing process [20]. These phenomena cause an evolution of the material, and this change may be detected by the TFBG in refractometric terms by measuring small changes in the RI.

5. Conclusions

A TFBG sensor embedded in the silicone adhesive of a cover glass sandwich sample was demonstrated to be able to detect simultaneously strain-temperature and RI variations of the silicone material when the tested sample was exposed to high vacuum thermal cycles. The sensor used had a TR of 7 °C, a strain resolution of 5.02 με, a RI resolution of 2×10^{-7} and a normalised envelope area accuracy of 1.6×10^{-3}. Silicone strain variations could be calculated, avoiding the inconsistencies obtained from the temperature compensation of the TFBG spectrum through the TC measures due to the non-localized measurements for the different position of the two sensors. A substantial permanent negative strain (∼100 με) was measured by the self-compensated TFBG at the end of the test, implying the possibility of shrinkage effects due to the post-curing/ageing reactions occurring in the silicone during the thermal cycles. Another effect causing the occurrence of negative stress may be the difference between the CTEs of the used materials in contact and the sample, in particular the cover glass and the silicone adhesive. The sensor was able to detect also a variation of RI of the adhesive, suggesting that the thermal cycles performed in high vacuum induced an evolution of the silicone. Specifically, at the beginning, the silicone RI was 1.42648, while after the test it was 1.42744 at the same temperature. To specifically investigate this aspect, a DSC test was performed on a cured silicone sample, where the presence of volatiles released during the heating-up and the cooling-down was detected. The same phenomenon, but enhanced, is expected to occur during the vacuum thermal cycles test, which can be considered as the main cause of silicone RI changing. Therefore, the embedded TFBG sensor can provide information on the thermomechanical and refractometric state of the silicone during the high vacuum thermal cycles also in real-time.

Data availability statement

All data that support the findings of this study are included within the article (and any supplementary files).

Acknowledgments

We would like to thank our colleague Sarah Rodriguez for her contribution regarding the experiments performed in the thermal lab of ESTEC. This research was supported by ESA/ESTEC (visiting researcher programme) and the Operationeel Programma Zuid-Nederland (Op-Zuid) Project as part of the Dutch Composite Maintenance Centre (DCMC), supported by the Europees Fonds voor Regionale Ontwikkeling (EFRO) and the North Brabant province of the Netherlands. The views expressed herein can in no way be taken to reflect the official opinion of the European Space Agency (ESA) and are not intended to endorse particular technologies, companies, or products.

ORCID iDs

Luigi Fazzi https://orcid.org/0000-0001-6177-8615
Roger M Groves https://orcid.org/0000-0001-9169-9256

References

[1] Grossman E and Gouzman I 2003 Space environment effects on polymers in low earth orbit *Nucl. Instrum. Methods Phys. Res.* B **208** 48–57
[2] Kutz M 2018 *Handbook of Environmental Degradation of Materials* (Oxford: William Andrew Applied Science Publishers) p 736
[3] Fischer H R, Semprimoschnig C, Mooney C, Rohr T, van Eck E R H and Verkuijlen M H W 2013 Degradation mechanism of silicone glues under UV irradiation and options for designing materials with increased stability *Polym. Degrad. Stab.* **98** 720–6
[4] Banks B A, Rutledge S K, Sechkar E, Stueber T, Snyder A, de Groh K K, Haytas C and Brinker D 2000 *Proc. 8th Int. Symp. on Materials in a Space Environment, 5th Int. Conf. on Protection of Materials and Structures from the LEO Space Environment*
[5] Dever J A, Bruckner E J, Scheiman D A and Stidham C R 1994 *18th Aerospace Ground Testing Conf.* pp 94–2627
[6] Edwards D L, Tighe A P, Van Eesbeek M, Kimoto Y and de Groh K K 2010 Overview of the natural space environment and ESA, JAXA, and NASA materials flight experiments *MRS Bull.* **35** 25–34
[7] Alberto N, Marques C, Pinto J L and Nogueira R N 2010 Three-parameter optical fiber sensor based on a tilted fiber Bragg grating *Appl. Opt.* **49** 6085–91
[8] Fazzi L, Valvano S, Alaimo A and Groves R M 2021 A simultaneous dual-parameter optical fibre single sensor embedded in a glass fibre/epoxy composite *Compos. Struct.* **270** 114087

[9] Gu Q G and Zhou Q L 1998 Preparation of high strength and optically transparent silicone rubber *Eur. Polym. J.* **34** 1727–33
[10] Tyng L Y, Ramli M R, Othman M B H, Ramli R, Ishak Z A M and Ahmad Z 2013 Effect of crosslink density on the refractive index of a polysiloxane network based on 2,4,6,8-tetramethyl-2,4,6, 8-tetravinylcyclotetrasiloxane *Polym. Int.* **62** 382–9
[11] McIntosh K R, Cotsell J N and Cumpston J S 2008 *Proc. European PVSEC* pp 3475–82
[12] Hubera C, Steina B and Kalta H 2017 Plasma-enhanced chemical vapor deposition of amorphous silicon carbonitride: deposition temperature dependence of bonding structure, refractive index, mechanical stress and their aging under ambient air *Thin Solid Films* **634** 66–72
[13] Albert J, Shao L and Caucheteur C 2013 Tilted fiber Bragg grating sensors *Laser Photonics Rev.* **7** 83–108
[14] Fazzi L and Groves R M 2021 *Optics* 1247098
[15] Fazzi L and Groves R M 2020 Demodulation of a tilted fibre Bragg grating transmission signal using α-shape modified Delaunay triangulation *Measurement* **166** 108197
[16] Laffont G and Ferdinand P 2001 Tilted short-period fibre-Bragg-grating-induced coupling to cladding modes for accurate refractometry *Meas. Sci. Technol.* **12** 765–70
[17] avantor science Data-sheet of Nusil CV16-2500 (Available at: www.avantorsciences.com/nusil/en/product/CV16-2500/controlled-volatility-silicone-elastomer) (Accessed 21 September 2021)
[18] Dugas J, Michel P, Martin L and Cariou J M 1996 Behavior of the refractive index and of the coefficient of thermal expansion of silicone with temperature *Appl. Opt.* **25** 3807–8
[19] De Heer J 1957 The principle of Le Châtelier and Braun *J. Chem. Educ.* **34** 375
[20] White C, Tan K, Wolf A and Carbary L 2010 Advances in structural silicone adhesives *Advances in Structural Adhesive Bonding* Woodhead Publishing Series in Welding and Other Joining Technologies (Cambridge: Woodhead Publishing) ch 4 pp 66–95